Journal of Neuroscience Research

Journal of Neuroscience Research 88:2940–2951 (2010)

Inhibition of Neutral Sphingomyelinase-2 Perturbs Brain Sphingolipid Balance and Spatial Memory in Mice

Nino Tabatadze,[1] Alena Savonenko,[2] Hongjun Song,[1,3] Veera Venkata Ratnam Bandaru,[1] Michael Chu,[1] and Norman J. Haughey[1]*

[1]Department of Neurology, The Johns Hopkins University School of Medicine, Baltimore, Maryland
[2]Department of Pathology, The Johns Hopkins University School of Medicine, Baltimore, Maryland
[3]The Institute for Cell Engineering, The Johns Hopkins University School of Medicine, Baltimore, Maryland

The sphingolipid ceramide is a bioactive signaling lipid that is thought to play important roles in modulating synaptic activity, in part by regulating the function of excitatory postsynaptic receptors. However, the molecular mechanisms by which ceramide exerts its effects on synaptic activity remain largely unknown. We recently demonstrated that a rapid generation of ceramide by neutral sphingomyelinase-2 (nSMase2; also known as "sphingomyelin phosphodiesterase-3") played a key role in modulating excitatory postsynaptic currents by controlling the insertion and clustering of NMDA receptors (Wheeler et al. [2009] J. Neurochem. 109:1237–1249). We now demonstrate that nSMase2 plays a role in memory. Inhibition of nSMase2 impaired spatial and episodic-like memory in mice. At the molecular level, inhibition of nSMase2 decreased ceramide, increased PSD-95, increased the number of AMPA receptors, and altered the subunit composition of NMDA receptors. Our study identifies nSMase2 as an important component for efficient memory formation and underscores the importance of ceramide in regulating synaptic events related to learning and memory.

Key words: memory; NMDA; AMPA; ceramide; synapse; sphingomyelinase

It is becoming increasingly well recognized that lipids play critical roles in regulating neuronal excitability. The biophysical properties of lipids regulate shape, endo- and exocytotic events, and vesicle and protein trafficking, and considerable numbers of lipid species also function as second messengers that regulate a multitude of neuronal events (Swartz, 2008; Day and Kenworthy, 2009; Owen et al., 2009; Stahelin, 2009). Given the potential importance of lipids in regulating neuronal functions, relatively little is known about the mechanisms by which lipids control synaptic events.

Sphingolipids are a class of lipid especially enriched in the central nervous system. The sphingolipid ceramide is a bioactive lipid that modulates a variety of cellular events ranging from proliferation to apoptosis (van Blitterswijk et al., 2003; Claus et al., 2009). Ceramide can be rapidly generated in focal compartments by the actions of a family of sphingomyelin-catabolizing enzymes, the sphingomyelinases. There are three general classes of sphingomyelinase, which based on their pH optima are categorized as neutral, acidic, and alkaline sphingomyelinases. Three neutral sphingomyelinases (nSMase2–4) have been identified and cloned (Schneider and Kennedy, 1967; Tomiuk et al., 1998; Hofmann et al., 2000; Mizutani et al., 2000). nSMase2 is highly enriched in the neurons of hippocampus and dentate gyrus (Rao and Spence, 1976; Hofmann et al., 2000), suggesting that it may play a role in hippocampus-dependent memory. Indeed, several lines of evidence suggest that ceramide generated by nSMase2 is important for regulating synaptic activities related to memory. Nerve growth factor (NGF)-induced neurite outgrowth and synaptogenesis are regulated by nSMase2 and its reaction product ceramide (Ito and Horigome, 1995; Brann et al., 1999; Hirata et al., 2001), and NGF-induced activation of nSMase2 can rapidly enhance the rate of depolarization-induced action potentials (Zhang et al., 2002; Zhang and Nicol, 2004; Nicol, 2008). Recently, we demonstrated that tumor necrosis factor-α (TNFα)-induced enhancement of excitatory postsynaptic currents and NMDA-evoked calcium bursts were regulated by nSMase2-mediated generation of ceramide

Additional Supporting Information may be found in the online version of this article.

Contract grant sponsor: NIH; Contract grant number: MH077542; Contract grant number: AA0174078 (to N.J.H.); Contract grant number: AG24984 (to H.S., N.J.H.).

*Correspondence to: Norman J. Haughey, Department of Neurology, The Johns Hopkins University School of Medicine, Meyer 6-109, 600 North Wolfe Street, Baltimore, MD 21287. E-mail: nhaughe1@jhmi.edu

Received 18 November 2009; Revised 26 February 2010; Accepted 23 April 2010

Published online 13 July 2010 in Wiley Online Library (wileyonlinelibrary.com). DOI: 10.1002/jnr.22438

(Wheeler et al., 2009). Similar effects at postsynaptic sites have been produced by direct additions of synthetic cell-permeable ceramide analogs that increase excitatory postsynaptic currents without affecting paired-pulse facilitation (Furukawa and Mattson, 1998; Coogan et al., 1999; Fasano et al., 2003). These ceramide-associated enhancements of excitatory currents are often transient and are followed by sustained depression of excitatory postsynaptic currents (Furukawa and Mattson, 1998; Coogan et al., 1999; Yang, 2000; Davis et al., 2006; Tabarean et al., 2006). Combined, these findings support complex roles for sphingolipids in regulating neuronal excitability that may in part depend on the spatial and temporal production of ceramide. Despite these physiological and biochemical findings suggesting that ceramide generated by nSMase2 may be important for synaptic events related to learning and memory, a role for nSMase2 in memory has not been established. Here we provide evidence that nSMase2 is important for spatial and episodic-like memory in mice and uncover roles for nSMase2 in the constitutive regulation of brain ceramide metabolism and postsynaptic structure.

MATERIALS AND METHODS

Animals

Mice with a deletion in the gene encoding nSMase2 were kindly provided by Dr. Christophe Poirier. These mice exhibit a complete loss of nSMase2 activity as described previously (Aubin et al., 2005). Because mutation in nSMase2 produces dwarfism and defects of osteogenesis that could interfere with behavioral training (Aubin et al., 2005; Stoffel et al., 2005, 2007), the use of these mice was restricted to biochemical analysis of brain sphingolipid content. Behavioral testing required 14 consecutive days of training, so it was not practical to administer GW4869 directly into brain, because this number of repeated injections is very likely to induce local inflammation and tissue damage. Therefore, we used the nSMase2-specific inhibitor GW4869 (Haughey et al., 2004; Kolmakova et al., 2004; Marchesini and Hannun, 2004; Peng et al., 2006; Smith et al., 2006; Takahashi et al., 2006; Walton et al., 2006). Male C57BL/6J mice (4 months old) were injected intraperitoneal once daily with GW4869 (1.25 mg/kg, dissolved in saline with 2.5% dimethylsulfoxide; Calbiochem, Gibbstown, NJ) 7 days prior and during behavioral testing for a total of 21 daily injections. An experimental timeline is included in Supporting Information Figure 1. In preliminary experiments, we determined that this dose of GW4869 did not produce any adverse effects, did not alter the sphingomylein or ceramide content of heart, skeletal muscle, or liver (Supp. Info. Fig. 2), and did enter into brain in sufficient quantity to inhibit neutral sphingomyelinase activity (see Fig. 1). Control mice were injected with the vehicle used to dissolve GW4869 (2.5% dimethylsulfoxide). All animals were housed in groups of five and maintained on 12 hr light-dark cycle with free access to water and rodent chow. Behavioral training consisted of the following memory paradigms. A classic version of the Morris water maze, repeated reversals task, radial water maze, and Y maze. On the last day of training, all animals were sacrificed and brains rapidly removed. Brains were dissected with a sagittal incision down the center line, and one half was immersed in 4% paraformaldahide and stored at 4°C for 5 days, followed by postfixation in 30% sucrose for 48 hr. The remaining tissue was rapidly dissected into cortex, hippocampus, striatum, and cerebellum and snap-frozen. Frozen brain tissues were stored at –80°C. All rodent procedures were conducted according to NIH guidelines for animal care and were approved by the JHU Institutional Animal Care and Use Committee.

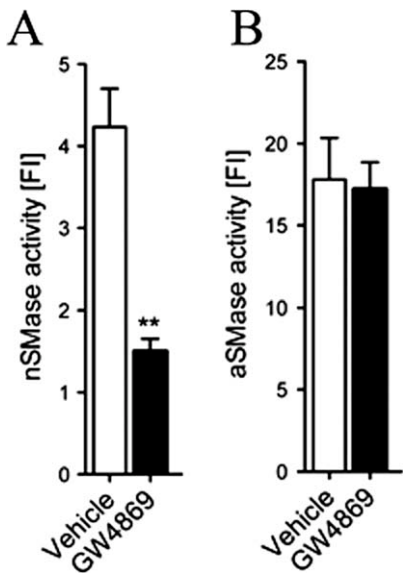

Fig. 1. Intraperitoneal administration of GW4869 decreases nSMase activity in brain. **A:** Summary data showing a significant reduction of neutral sphingomyleinase activity in cortex of mice treated with GW4869 for 21 consecutive days compared with vehicle-injected controls. **B:** Acid sphingomyelinase activity was similar in cortex of GW4869- and vehicle-administered mice (n = 12 treated with GW4869, 13 treated with vehicle). $^{**}P < 0.01$ one-way ANOVA. Values represent mean ± SD.

Pretraining

Mice were handled daily for 5 days to acclimate them to investigator handling. On the sixth day, mice were pretrained in a small pool (diameter 55 cm) with a platform (10 × 10 cm) submerged 1 cm below the water surface as previously described (Savonenko et al., 2005). Mice were placed in the water facing the platform and allowed to swim, climb on the platform, and stay there for 10 sec. Mice were then removed from the platform, dried, and returned to a dry waiting cage for 10–12 min. In total, six trials were performed during the pretraining session.

Classic Morris Water Maze and Repeated Reversals

A fixed-platform version of the water maze paradigm was carried out as previously described (Savonenko et al., 2005). Briefly, mice were trained in a 100-cm-diameter pool filled with opaque water (21°C ± 2°C) and surrounded by various visual cues. A collapsible platform (10 × 10 cm) was

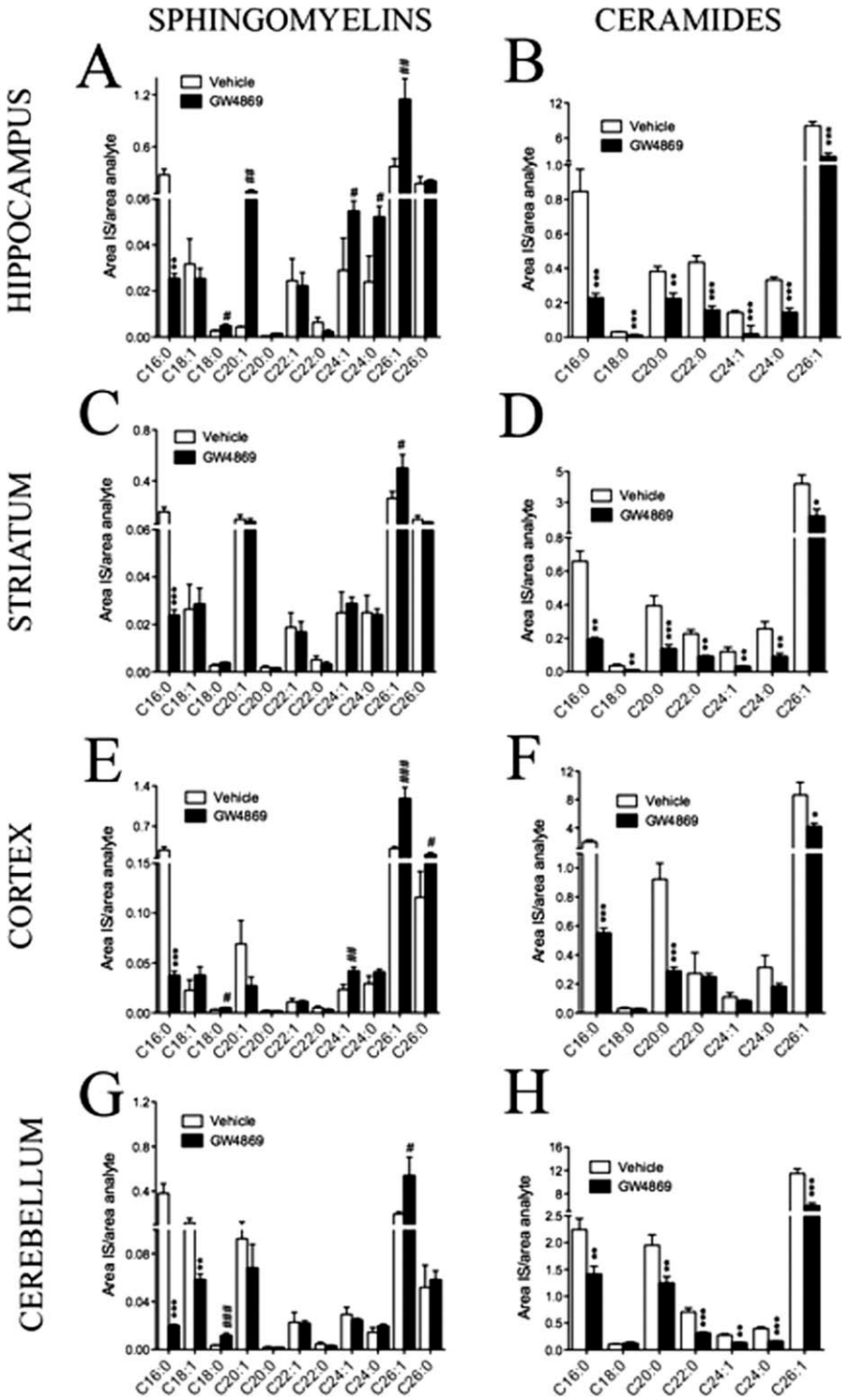

Fig. 2. Inhibition of nSMase2 modifies brain sphingolipid content. Brain levels of most sphingomylein species were increased and most ceramides species decreased following long-term inhibition of nSMase2. Summary data showing the effects of inhibiting nSMase2 on sphingomyelin and ceramide content of hippocampus (**A,B**), striatum (**C,D**), cortex (**E,F**), and cerebellum (**G,H**; n = 12 treated with GW4869, 13 treated with vehicle). $^{*}P < 0.05$, $^{**}P < 0.01$, $^{***}P < 0.001$ decreased compared with control, $^{\#}P < 0.05$, $^{\#\#}P < 0.01$, $^{\#\#\#}P < 0.001$ increased compared with control. ANOVA with Tukey post hoc comparisons. Values represent mean ± SD.

submerged 1 cm below the water surface in one of the four quadrants and remained in the same position until the end of the training. The starting location for each trial was randomly altered among three quadrants. The maximum duration of each trial was 60 sec, and mice that failed to find the platform during this time were guided to the platform and then removed. Mice were given 12 trials per day for 5 consecutive days, including one probe trail at the beginning and a second probe trial at the end of each training session. The platform was completely submerged during probe trials, and the mouse was allowed to swim freely for a variable time interval (30–45 sec). During probe tests, the percentage of time spent in annuli (area surrounding the platform, 20 and 40 cm in diameter) was recorded. At the end of the probe trial, the platform was raised and the mouse was allowed to escape onto the platform to avoid extinction resulting from repeated probe trials. Performance in all tasks was recorded using an HVS video tracking system (HVS Image Analysis VP-200; HVS, Hampton, United Kingdom). After completion of a classic Morris water maze, mice were trained in a repeated reversals paradigm for 2 days as previously described (Savonenko et al., 2005). This task differs from the classic water maze by changing the platform location at the start of each day. In this paradigm, mice are required to inhibit memory for the old platform location and learn the new location. Latency (time spent to locate the hidden platform from the start location) and swim speed (average speed during a trial) were measured during the platform trials. In the probe trials, percentage of time spent in the area 20 cm in diameter around the platform was recorded (annulus 20).

Radial Water Maze

The radial arm water maze task was conducted as previously described (Savonenko et al., 2005). A six-arm radial maze made of clear plastic was placed into the pool, and the platform was submerged at the end of one arm. The platform location was randomly changed between different arms at the beginning of each training day. The start position was located at the end of one arm and was randomly chosen in every trial. Mice were given six trials per day for 4 consecutive days. The maximum duration for each trial was 120 sec, and mice that did not find the platform were guided to the platform by experimenter, allowed to stay on the platform for 10 sec, and then moved to the waiting cage. Latency to find the platform and the number of correct arm entries where the platform was located on the previous day were registered and analyzed.

Y Maze

The Y maze test was conducted in a wooden, elevated, Y-shaped maze according to previously established protocols (Melnikova et al., 2006), with minor modifications. Mice performed a two-trial Y maze task in which one arm was blocked during the first trial using a stable barrier. Mice were placed at the end of one arm and allowed to explore the maze for 5 min, and the sequence of arm entries was recorded. After a 30-min rest interval, trial 2 began by placing mice at the end of one arm with all three arms opened and available for exploration. A two-trial Y-maze task represents a classic test for spatial recognition memory. Mice with intact memory have a tendency to explore novel arm more often than the rest of the maze, whereas mice with memory impairment enter all three arms evenly (Conrad et al., 1996; Dellu et al., 1997). The number of visits to the novel arm was calculated for a 5-min duration of testing. Motor activity was assessed on the basis of total number of arms visited during each trial. Spontaneous alternation behavior was calculated as the number of triads containing entries into all three arms divided by the maximum number of possible alternations.

Sphingomyelinase Activity Assay

The Amplex red sphingomyelinase assay kit (Molecular Probes, Eugene, OR) was used to quantify acid- and neutral sphingomyelinase activities according to the manufacturer's protocols. Assays were conducted with 50 μg of cortical tissue. Cortical homogenates were incubated for 30 min at 37°C in 100 μl of working solution that consisted of 2 U/ml HRP, 0.2 U/ml choline oxidase, 8 U/ml alkaline phosphatase, and 0.5 mM sphingomyelin. Neutral sphingomyelinase activity was determined in working buffer with a pH of 7.4. Acidic sphingomyelinase activity was measured by first adjusting the pH of the working solution to 5.0 during incubation, then increasing the pH to 7.4 to allow for detection of the product with the Ampex red reagent. The reaction product was measured using a fluorescent plate reader (absorption at 571 nm and emission at 585 nm; SpectraMax M2e; Molecular Devices, Sunnyvale, CA). Positive controls consisted of sphingomyelinase (40 U/ml) or H_2O_2 (20 mM) added to the working solution.

Immunoblotting

For Western blots, cortical tissues were homogenized in ice-cold buffer containing 20 mM Tris-HCl (pH 7.4), 50 mM NaF, 0.32 M sucrose, 2 mM EDTA, 2 mM EGTA, 0.2 mM sodium orthovanadate, 1 mM PMSF, and protein inhibitor cocktail (Roche Diagnostics GmbH, Mannheim, Germany). Proteins (10 μg of total protein per lane) were separated by sodium dodecyl sulfate-polyacrylamide gel electrophoresis and transferred to nitrocellulose membranes. Membranes were blocked in Tris-buffered saline (TBS) containing 10 mM Tris-HCl, pH 7.4, 150 mM NaCl and 0.1% Tween 20 (TBS-T) for 1 hr and incubated with primary antibodies overnight at 4°C. Monoclonal antibodies included PSD-95 (1:5,000; Oncogene, Cambridge, MA), synaptophysin (1:1,000; Sigma, St. Louis, MO), NR1 (1:1,000; Calbiochem), NR2A (1:1,000; Calbiochem), NR2B (1:1,000; Calbiochem), GluR1 (1:1,000; Millipore, Billerica, MA), GluR2 (1:1,000; Millipore), GluR3 (1:1,000; Cell Signaling Technology, Danvers, MA), and β-actin (1:1,000; Sigma). After incubations with primary antibodies, membranes were washed in TBS and TBS-T and incubated at room temperature for 1 hr with HRP-conjugated secondary antibodies (1:5,000; goat anti-mouse IgG; 1:5,000; goat anti-rabbit IgG; Promega, Madison, WI). Immunoreactivity was visualized using Pico West Super-Signal (Pierce, Rockford, IL), and optical densities were quantified in NIH ImageJ software.

Immunohistochemistry and Immunofluorescent Staining for Free-Floating Sections

Coronal sections (30 μm) were washed in TBS three times and incubated in 1% hydrogen peroxide for 30 min to block endogenous peroxidase activity. Tissue sections were then washed three times in T-TBS and blocked for 1 hr in 5% normal goat serum. Rat anti-mouse neutrophil primary antibody was added (1:1,000; Serotec, Raleigh, NC) and incubated overnight on shaking platform at 4°C. Tissue sections were then washed in T-TBS and incubated in biotinylated secondary antibody (1:300; Bio-Rad, Hercules, CA) for 1 hr at room temperature and incubated for 30 min in ABC kit reagent mixture in order to form biotin-avidin complexes (Vectastain ABC kit; Vector Laboratories, Burlingame, CA). Tissue sections were then briefly rinsed and stained with diaminobenzidine (DAB) according to the manufacturer's directions (Vector Laboratories). Stained sections were mounted on slides and coverslipped with Permount clear mounting media (Sigma). For immunofluorescent staining, the following primary antibodies were used: polyclonal anti-Iba (1:1,000; Wako Chemicals, Richmond, VA), polyclonal anti-GFAP (1:1,000; Dako, Carpinteria, CA). Seconday antibidies were Alexa fluor 488 and Alexa fluor 495 (both 1:500; Invitrogen, Carlsbad, CA). Images were obtained with a Zeiss microscope equipped with a Retiga 2000R Fast 1394 camera (QImaging, Surrey, British Columbia, Canada). Fluorescent intensity was quantified in Openlab software (Improvision, Waltham, MA).

Lipid Extraction and Measurement of Sphingolipids Using LC-ESI/MS/MS

Total lipids were extracted according to a modified Bligh and Dyer procedure (Shaikh, 1994), as described previously (Bandaru et al., 2007). Each sample was homogenized in 10 volumes of deionized water, then in 3 volumes of 100% methanol containing 30 mM ammonium acetate. The mixture was vortexed, and four volumes of chloroform was added, vortexed, and centrifuged at 1,000*g* for 10 min. The chloroform layer was removed, dried, and stored at –80°C until use. Samples were resuspended in 100% methanol for LC/MS/MS. Sphingomyelins and ceramides were detected and quantified using multiple reaction monitoring (MRM). Samples were injected with a PAL autosampler into a PerkinElmer HPLC equipped with a C18 column (100 × 2 mm, 5 μm) coupled to the guard column containing identical packing material (Phenomenex, Torrance, CA). For a typical run, the LC column was first preequilibrated for 0.5 min with the first mobile phase consisting of 85% methanol, 15% H_2O, and 5 mM ammonium formate. The column was then eluted with the second mobile phase consisting of 99% methanol, 1% formic acid, and 5 mM ammonium formate at the flow rate of 100.0 μl/min. The eluted sample was injected into the ion source, and the detection and quantitation of each analyte were carried out by LC/MS/MS in MRM mode, monitoring the parent compound and products by ion scan. Slight differences in the efficiency of extraction and fluctuations in the efficiency of mass detection were controlled for by normalizing data to the internal standards sphingomyelin C12:0 and ceramdie C12:0 (Avanti Polar Lipids, Alabaster, AL). Sphingomyelin and ceramide standards C16:0, C18:0, C18:1 were purchased from Sigma. Ceramides C20:0, C24:0, C24:1 were purchased from Avanti Polar Lipids. Palmitoyl-lactosyl ceramide C16:0-C16:0, stearoyl-lactosyl-ceramide C16:0-C18:0, lignoceryl-glucosyl-ceramide C16:0-C24:0, lignoceryl-galactosyl-ceramide C16:0-C24:0, and stearoyl-galactosyl-ceramide-sulfate C18:1-C24:0 were purchased from Matreya Inc. (Pleasant Gap, PA). Data were collected and processed in Analyst 1.4.2 software.

Statistical Analyses

Behavioral data were analyzed bgy using repeated-measures or main-effect ANOVAs, with a minimal level of significance of $P < 0.05$. Post hoc Tukey tests were applied to significant differences in repeated-measures ANOVAs. One-way ANOVA and nonpaired *t*-tests were used to assess differences in sphingolipid and synaptic protein levels.

RESULTS

Inhibition of Neutral Sphingomyelinase-2 Disrupts Brain Ceramide-Sphingomylein Balance

Genetic models of mutation or deletion in nSMase2 result in defects of bone formation (Aubin et al., 2005; Stoffel et al., 2005, 2007) and were consequently not appropriate for behavioral testing that requires intact locomotor activity. Therefore, we employed a pharmacological approach using GW4869, a selective inhibitor of nSMase2 (Luberto et al., 2002). We first determined whether systemically administered GW4869 entered brain in sufficient amounts to inhibit nSMase2. We found that GW4869 decreased neutral sphingomyelinase activity in cortex by 64.3% (Fig. 1A). Treatment with GW4869 did not affect acidic sphingomyelinase activity (Fig. 1B), which is consistent with data from previous reports showing that this drug specifically targets nSMase2 (Haughey et al., 2004; Kolmakova et al., 2004; Marchesini and Hannun, 2004; Peng et al., 2006; Smith et al., 2006; Takahashi et al., 2006; Walton et al., 2006). Because nSMase2 catalyzes the hydrolysis of sphingomyelin to ceramide, we next determined whether inhibition of nSMase2 by GW4869 affected brain sphingolipid content. Treatment with GW4869 decreased multiple species of ceramide and increased multiple species of sphingomyelin in all brain regions examined (Fig. 2A–H), with the exception of sphingomyelin C16:0, which was decreased in all brain regions (Fig. 2A,C,E,G). These results are strikingly similar to those obtained by analysis of sphingomyelin and ceramide content in brain tissues from mice containing a deletion mutation in the nSMase2 gene (Supp. Info. Fig. 2), further confirming the specificity of GW4869 for nSMase2. There were no significant changes of ceramide or sphingomyelin levels in liver, kidney, heart, or skeletal muscle of mice treated with GW4869 compared with control mice administered vehicle (data not shown). Unexpectedly, we found that treatment with GW4869 altered the sphingolipid content of serum in a direction opposite to what we observed in brain tissue. In serum,

treatment with GW4869 increased multiple ceramides and decreased multiple sphingomyelins, with few exceptions (Fig. 3A,B). Based on evidence that ceramide can play important roles in the activation of monocytes (Sipka et al., 2000; Detre et al., 2006), we next we next determined whether GW4869 altered the trafficking of monocytes into brain parenchyma or activated brain resident glia. GW4689 did not alter the number or morphology of Iba-1-immunopositive marcophage/microglia or GFAP-immunopositive astrocytes or the number of immunopositive neutrophils (Supp. Info. Fig. 3), indicating that inhibition of nSMase2 did not alter the CNS trafficking of blood-derived monocytes or activation state of brain-resident glia.

Inhibition of nSMase 2 Impairs Early Phases of Spatial Reference Memory

Spatial reference memory was tested in a classic version of the Morris water maze beginning 7 days after the initiation of GW4869 treatment. Inhibition of nSMase2 with GW4869 did not affect daily averaged latencies to locate the hidden platform. There was a significant effect of day, indicating that both groups had progressively decreased latencies to locate the hidden platform with repeated training (Fig. 4A). There were no group differences in swimming speed (Fig. 4A, inset). A trial-by-trial analysis of the first training day showed that, whereas vehicle-treated mice had progressively decreased latencies to locate the hidden platform, mice treated with GW4869 failed to show decreased latencies to locate the platform with repeated trials (Fig. 4B). These differences were not due to an effect of treatment on swimming speed (determined for each trial during the first day of training; data not shown).

An analysis of the time spent in quadrants (target, adjacent left, adjacent right, and opposite) during the probe test at the end of the first training day indicated that mice treated with GW4869 spent less time searching in the target quadrant compared with mice administered vehicle. Furthermore, mice treated with GW4869 spent less time in the area surrounding the hidden platform (annulus 20) compared with mice administered vehicle (Fig. 4C,D). Both groups of mice spent equal time in the target quadrant (annulus 20) during the final probe trial performed at the end of the fifth training day (Fig. 4C,E). These data indicate that inhibition of nSMase2 delayed the formation of spatial reference memory in mice.

After 5 days of training in a classic Morris water maze task, mice were trained in a repeated reversals paradigm for 2 days to test episodic-like memory. In this setting, the hidden platform location was changed each day, and mice were required to learn the new platform location quickly while inhibiting memory for the previous location. Performance in the repeated reversals paradigm was not different in mice treated with GW4869 compared with vehicle controls (data not shown), suggesting that inhibition of nSMase2 does not affect episodic-like memory in mice.

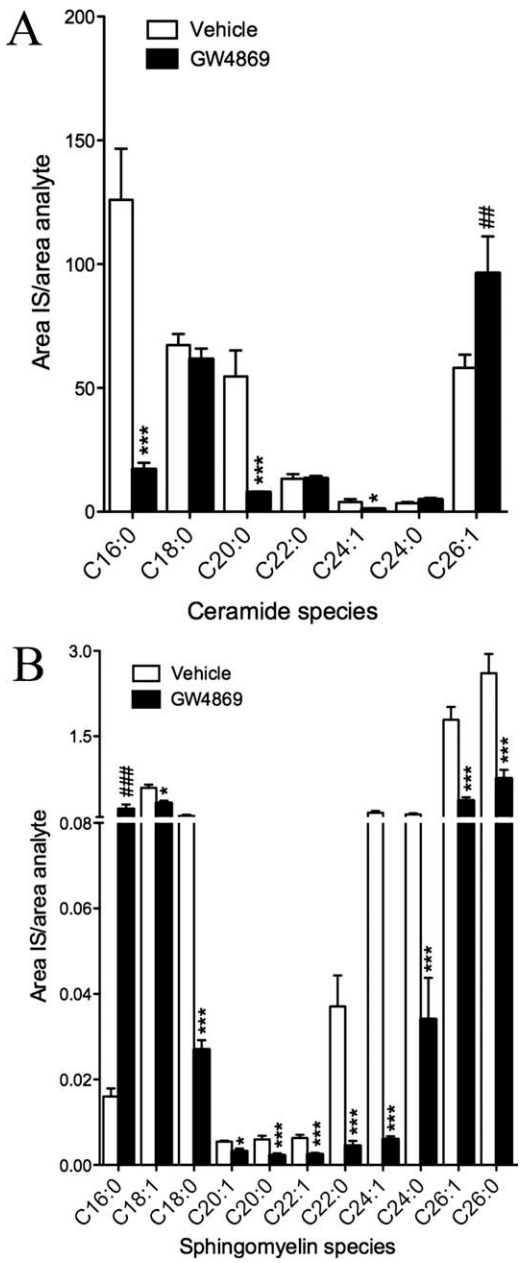

Fig. 3. Inhibition of nSMase2 modifies serum levels of ceramide and sphingomyelin. Long-term inhibition of nSMase2 decreased ceramide and increased sphingomylein in serum. Effects of inhibiting nSMase2 on serum ceramides (**A**) and sphingomyelins (**B**; n = 12 treated with GW4869, 13 treated with vehicle). $^{*}P < 0.05$, $^{***}P < 0.001$ greater than vehicle, $^{\#\#}P < 0.01$, $^{\#\#\#}P < 0.001$ less than vehicle. Two-way ANOVA with Tukey post hoc comparisons.

To assess episodic-like working memory, a six-arm radial maze enclosure was placed into the pool, and the platform location was changed daily so that mice were required to learn a new platform location every day. Latencies to locate the hidden platform during trial 1 on all 4 training days were similar in the two groups (Fig. 4F). Treatment with GW4869 significantly increased

latencies to locate the hidden platform during trials 2–5 across all 4 training days (Fig. 4F). To confirm that inhibition of nSMase2 interfered with episodic-like memory, we next analyzed the number of correct arm entries. The numbers of correct arm entries during trial 1 of training day 1 (defined as the arm corresponding to the quadrant where the platform was located on the last day of the repeated reversal task) were similar in the two groups and were not different from chance (chance level is 16%; Fig. 4G). On training day 2, mice treated with vehicle demonstrated long-term memory for the previous episode of training by visiting the correct arm 44% of the time, whereas mice treated with GW4869 visited the correct arm only 25% of the time; a frequency not significantly different from chance. These data indicate that inhibition of nSMase2 interfered with the formation of episodic-like working memory.

We next used a Y maze task to assess spatial recognition memory. Performance on this task was not different in mice treated with GW4869 compared with mice administered vehicle (data not shown), suggesting that spatial recognition memory was not altered by inhibition of nSMase2.

Long-Term Inhibition of nSMase2 Disrupts Synaptic Structure

Because synaptic organization is important for learning and memory, we measured several structural and functional synaptic proteins to determine whether inhibition of nSMase2 and dysregulation of brain sphingolipid balance modified synapses. Treatment with GW4869 increased the postsynaptic protein PSD-95, without affecting levels of the presynaptic protein synaptophysin (Fig. 5A,B). GW4869 did not alter levels of the NMDA receptor subunit NR1, indicating that inhibition of nSMase2 did not alter the total number of NMDA receptors. In mice treated with GW4869, there were increases in NR2A subunits but not NR2B, suggesting that inhibition of nSMase2 modified the subunit composition of NMDA receptors (Fig. 5C,D). The AMPA receptor subunit GluR1 was increased in mice treated with GW4869, indicative of an increase in the total number of AMPA receptors. Levels of AMPA receptor subunits GluR2 and GluR3 were similar in mice treated with GW4869 and mice administered vehicle (Fig. 5E,F). Combined, these data suggest that dysregulation of brain sphingolipid balance following inhibition of nSMase2 modified synaptic structure by increasing PSD95, altering the subunit composition of NMDA receptors, and increasing the number of AMPA receptors. These synaptic changes may account for defects of memory following long-term inhibition of nSMase2.

DISCUSSION

We have demonstrate here that nSMase2 is important for hippocampus-based memory. At the molecular level, inhibition of nSMase2 increased sphingomylein and decreased ceramide content in brain, increased PSD-95 levels, increased the number of AMPA receptors, and modified the subunit composition of NMDA receptors at postsynaptic sites in the hippocampus. Combined, these findings suggest that impairment of memory by inhibition of nSMase2 involves a disruption in sphingomy-

Fig. 4. Inhibition of nSMase2 disrupts an early phase of memory. Inhibition of nSMase2 impaired spatial reference and episodic-like memory. **A:** Averaged daily latencies to locate the hidden platform in a classic version of Morris water maze were similar in mice treated with GW4869 or vehicle [two-way repeated measures (treatment × day) ANOVA, effect of treatment $F(1, 90) = 0.05$, $P > 0.8$; day $F(4, 90) = 26.6$, $P < 0.001$; and treatment-by-day interaction $F(4, 90) = 0.27$, $P > 0.8$]. **Inset** shows that treatment with GW4869 did not affect swimming speed (average of swim speed over all 5 days of training is shown; *t*-test, $P > 0.5$). **B:** Latencies to locate the hidden platform for each trial of training on day 1 showing that inhibition of nSMase2 impaired the ability of mice to learn the location of the hidden platform [two-way (treatment × trial) ANOVA for latency on the first day of training revealed significant effects of treatment $F(1, 230) = 2.49$, $P < 0.05$; trial $F(9, 230) = 2.22$, $P < 0.05$; and treatment-by-trial interaction $F(9, 230) = 3.63$, $P < 0.001$]. **C:** Occupancy plots for the probe trials performed at the end of training day 1 and training day 5. Increasing color intensity indicates the region where mice spent the most time during probe trials. Inhibition of nSMase2 with GW4869 significantly decreased the time mice spent in the region surrounding the platform (annuli 20 and 40) during the first probe trial. Although mice treated with GW4869 were not as accurate in remembering the platform location during the last probe trial, the time they spent in annulus 20 was not statistically different from that of mice treated with vehicle. Annuli representing the area of 20- and 40-cm diameters around the platform are indicated in concentric blue circles. **D,E:** Quantitative data showing the time spent in annulus 20 during the first (P1) and last (P2) probe trials [two-way (treatment × quadrant) ANOVA for the first probe test showed significant effect of treatment $F(1, 92) = 5.35$, $P < 0.01$; quadrant $F(3, 92) = 10.73$, $P < 0.001$; and treatment-by-quadrant interaction $F(3, 92) = 7.79$, $P < 0.001$, Tukey post hoc for annulus 20, $P < 0.01$; two-way (treatment × quadrant) ANOVA for the last probe test did not show significant effect of treatment $F(1, 92) = 0.59$, $P > 0.4$; and there was an effect of quadrant in both groups $F(3, 92) = 60.03$, $P < 0.001$; and treatment-by-quadrant interaction was not significant $F(3, 92) = 0.002$, $P > 0.9$, Tukey post hoc for annulus 20, $P > 0.9$]. **F:** Averaged latencies for trials 2–6 across 4 days of training in a radial water maze. Mice treated with GW4869 showed longer latencies to locate the hidden platform during trials 2–5 across the 4 days of training [three-way ANOVA revealed a significant effect of treatment $F(1, 23) = 7.01$, $P < 0.05$; and trial $F(4, 92) = 53.80$, $P < 0.001$]. **G:** Summary data of correct arm entries in the radial water maze (a correct entry is recorded as entry into the arm where the platform was located on the previous day of training). On training day 2, mice treated with vehicle demonstrated long-term memory for the previous episode of training by visiting the correct arm more often than a chance level (chance level of 16% is indicated with a red line). Mice treated with GW4869 were unable to remember the previous platform location (ANOVA, $P < 0.01$; Tukey post hoc, $P < 0.01$). [Color figure can be viewed in the online issue, which is available at wileyonlinelibrary.com.]

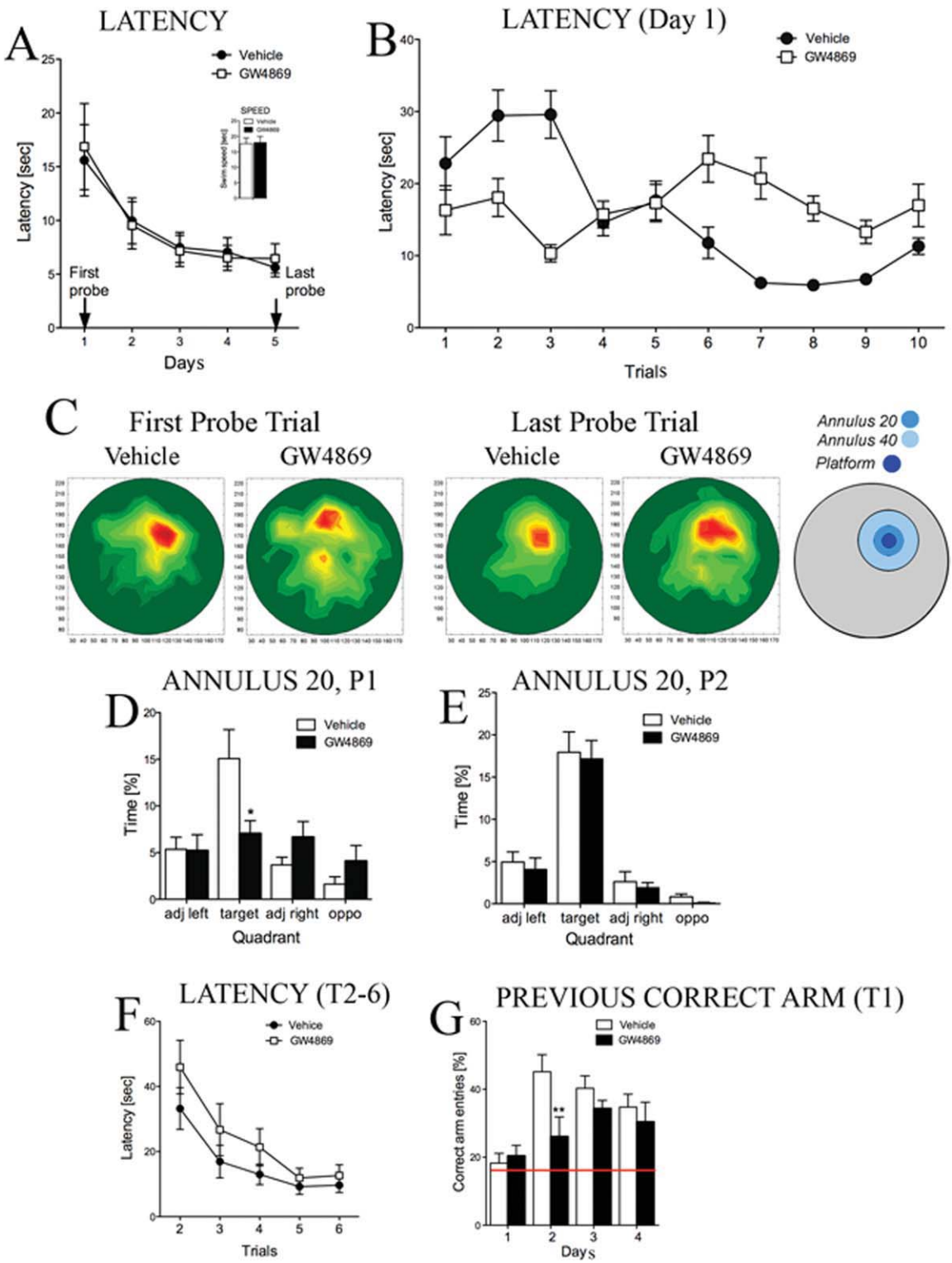
A
LATENCY
Vehicle
GW4869
SPEED
Latency [sec]
First probe
Last probe
Days
B
LATENCY (Day 1)
Vehicle
GW4869
Latency [sec]
Trials
C
First Probe Trial
Vehicle
GW4869
Last Probe Trial
Vehicle
GW4869
Annulus 20
Annulus 40
Platform
D
ANNULUS 20, P1
Vehicle
GW4869
Time [%]
adj left
target
adj right
oppo
Quadrant
E
ANNULUS 20, P2
Vehicle
GW4869
Time [%]
adj left
target
adj right
oppo
Quadrant
F
LATENCY (T2-6)
Vehicle
GW4869
Latency [sec]
Trials
G
PREVIOUS CORRECT ARM (T1)
Vehicle
GW4869
Correct arm entries [%]
Days

Figure 4.

elin/ceramide balance and dysregulation of postsynaptic glutamatergic signaling.

It is interesting that systemic administration of GW4869 did not alter the ceramide or sphingomylein content of liver, heart, or skeletal muscle but did decrease the ceramide content and increase the sphingomyelin content in brain. These findings suggest that nSMase2 may have a constitutive activity in CNS but is largely an inducible enzyme in peripheral tissues. These drug-induced changes in brain sphingolipid content were extremely similar to those observed in mice with a deletion mutation in nSMase2 gene, indicating that GW4869 effectively and specifically targeted nSMase2. The effects of GW4869 on sphingomyelin and ceramide content were most striking in the hippocampus, consistent with the high regional expression of nSMase2 in this brain structure (Hofmann et al., 2000). These findings not only indicate that GW4869 is an effective inhibitor of brain nSMase2 but further suggest that, in addition to the inducible actions of this sphingolipid-modifying enzyme (Clarke and Hannun, 2006), nSMase2 may be involved in the constitutive regulation of ceramide metabolism in brain.

Inhibition of nSMase2 with GW4869 slowed learning. Mice administered GW4869 did not progressively decrease latency to locate the hidden platform with repeated training trials, suggesting that they had difficulty learning to use spatial cues to navigate the pool. During the first probe test, mice administered GW4869 spent less time in the target area (measured by annulus surrounding the platform), further demonstrating that inhibition of nSMase2 interfered with spatial learning. Starting at day 2 of probe trials, latencies to locate the hidden platform in mice administered GW4869 were similar to vehicle, suggesting that inhibition of nSMase2 slows, but does not abolish, learning. Similarly, mice administered GW4869 were able to use the spatial navigation memory acquired in the classic Morris water maze in subsequent repeated reversals tasks. In this more challenging procedure, earlier locations of the platform have to be disregarded, and memory retrieval must be selective for the most recently encoded location; an ''episode-like'' component of the task. The repeated reversals task has close similarities to working-memory protocols in which the animal acquires information that is useful only for a given period (Steele and Morris, 1999). One possibility for why inhibition of nSMase2 did not interfere with performance on repeated reversal tasks is that nSMase2-dependent plasticity is important for procedural learning that is intrinsic to the acquisition of the Morris water maze (such as learning to use a platform as an escape location) but is not critical for episodic-like memory required for repeated reversals tasks. A second possibility is that prior learning with the Morris water maze influenced later learning on repeated reversal tasks. Indeed, previous studies have shown that pretraining mice in the water maze substantially ameliorated AP5-induced memory deficit despite a complete blockade of long-term potentiation (LTP; Bannerman et al., 1995; Nakazawa et al., 2004).

After repeated reversals tasks, mice were trained in the radial arm water maze. A delay in learning on day 2 of training in the radial arm water maze, similar to what was observed in the classic Morris water maze, was apparent in mice administered GW4869. Compared with the classic water maze, the radial arm water maze has different geometry and is a more challenging task that invokes a broad range of synaptic activation within hippocampal neuronal networks, which may not involve networks not active during classic water maze or repeated reversals tasks (Schwegler et al., 1996; Crusio and Schwegler, 2005). These findings corroborate observations in the classic water maze that inhibition of nSMase2 slows, but does not abolish, spatial learning. We cannot, however, rule out the possibility that nSMase2 is also important for other types of memory.

Sphingolipids are thought to play important roles in neuronal communication by modulating synaptic strength and connectivity. The nSMase2 belongs to a family of enzymes that cleave the phosphodiester linkage of sphingomyelin to create ceramide and phosphocholine. The rapid kinetics and location of nSMase2 make it a likely candidate to be involved in the modulation of plasticity in the CNS. nSMase2 can be rapidly activated, with peak activity in 1–2 min, and is highly expressed in the central nervous system, where expression is prominent in large neuronal cells, including Purkinje cells, pyramidal cells, neurons of the dentate gyrus granular layer, and pontine nuclei (Hofmann et al., 2000). At the presynaptic terminal, a rapid generation of ceramide is thought to enhance the rate of synaptic transmitter release by facilitating the trafficking and fusion of synaptic vesicles with the plasma membrane (Bajjalieh et al., 1989; Rohrbough et al., 2004; Rogasevskaia and Coorssen, 2006). Preventing rapid ceramide generation by inhibition of sphingomyelinases blocks calcium-induced glutamate release in cerebellar neurons (Numakawa et al., 2003). At the postsynaptic membrane, ceramide appears to play complex roles in modulating neuronal excitability. Ceramide analogs and the endogenous generation of ceramide have been shown rapidly to enhance excitatory postsynaptic currents (Furukawa and Mattson, 1998; Yu et al., 1999; Zhang et al., 2002; Fasano et al., 2003; Wheeler et al., 2009), which is often followed by sustained depression of synaptic currents (Coogan et al., 1999; Furukawa and Mattson, 1998; Yang, 2000; Tabarean et al., 2006; Davis et al., 2006). It has also been demonstrated in vivo that intraperitoneal administration of the ceramide analog PDMP restored synaptic function and preserved spatial memory in ischemic rats (Inokuchi et al., 1997; Yamagishi et al., 2003). Although the exact molecular mechanisms for the effects of ceramide on neuronal excitability are not yet fully understood, we recently demonstrated that a rapid production of ceramide by nSMase2 was required for TNFα-induced insertion of NMDA receptors into postsynaptic membranes and enhancement.

One mechanism by which sphingolipids may regulate synaptic plasticity is by controlling the location and

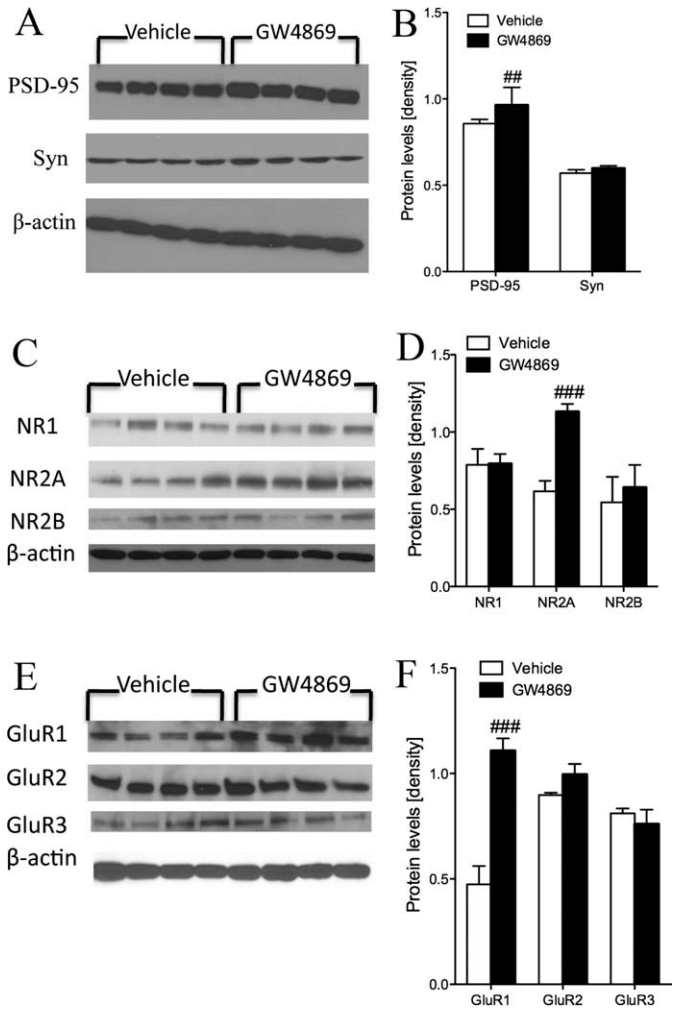

Fig. 5. Perturbation of brain sphingolipid content disrupts synaptic integrity. **A,C,E:** Representative Western blots showing the effects of long-term inhibition of nSMase2 on PSD-95, synaptophysin, and NMDA and AMPA receptor subunits. **B,D,F:** Quantification of Western blot band intensities showing that inhibition of nSMase2 with GW4869 increased PSD-95 levels and increased the amount of NMDA receptor NR2A subunits and AMPA receptor GluR1 subunits. Quantitative data are the mean ± SD from 12 animals/group. $^{\#\#}P < 0.01$, $^{\#\#\#}P < 0.001$ greater than vehicle. Student's *t*-test.

trafficking of receptors at postsynaptic sites. Sphingomyelin, ceramide, cholesterol, and the ganglioside GM1 are key components of specialized membrane domains known as "lipid rafts." These highly ordered regions of membrane are thought to play important roles in receptor signaling by compartmentalizing membrane proteins into active focal signaling units and promoting cross-talk between different signaling cascades. In neurons, lipid rafts are important sites for docking and insertion of NMDA and AMPA receptors (Fullekrug and Simons, 2004; Besshoh et al., 2005; Wheeler et al., 2009). Disrupting lipid rafts by cholesterol depletion has been shown to reduce NMDA receptor currents and associated calcium flux and increased the basal internalization rate of AMPA receptors (Hering et al., 2003; Frank et al., 2004; Abulrob et al., 2005). Furthermore, pharmacological inhibition or a deletion mutation in nSMase2 prevented TNFα-induced insertion of NMDA receptors into lipid rafts, suggesting that some aspects of receptor trafficking may be regulated by enzymatic control of lipid composition. Our current findings further suggest that nSMase2 is an important component of the neuronal synapse. Long-term inhibition of nSMase2 increased sphingomyelin and decreased ceramide content in multiple brain regions (most notably in hippocampus) and modified synaptic structure. In this setting, PSD-95 increased, the number of AMPA receptors increased, and the subunit composition of NMDA receptors was altered. PSD-95 is a PDZ-domain-containing scaffolding protein that is located almost exclusively in the postsynaptic density of neurons. The amino-terminal region of PSD-95 contains three PDZ domains that are necessary and sufficient to localize PSD-95 to lipid rafts. PSD-95 is an essential synaptic adapter protein that is involved in anchoring NMDA and AMPA receptors. Overexpression of PSD-95 enhances dendritic spine maturation, increases the amplitude and frequency of AMPA receptor-mediated excitatory postsynaptic currents (EPSCs), and converts silent synapses into functional synapses by driving GluR1 into synapses (Husseini et al., 2000; Beique and Andrade, 2003; Stein et al., 2003; Ehrlich and Malinow, 2004). The PDZ1 domain of PSD-95 also binds to the NR2A subunit of NMDA receptors and is involved in increased insertion and decreased internalization of intact NMDA receptors (Lin et al., 2004). Interaction of PSD-95 and NR2A also regulates downstream signal transduction pathways, including CREB interaction with CRE promoter sites on target genes, to modulate transcriptional events related to neuronal connectivity and excitability (Deisseroth et al., 1999; Aarts et al., 2002; Gardoni et al., 2006; Chen et al., 2006; Sornarajah et al., 2008). Thus, it is likely that increased PSD-95 was directly associated with increases of GluR1 and NR2A and that these molecular events were involved in the perturbation of memory. Combined, our findings suggest that nSMase2 is important for memory, through actions that involve regulation of brain sphingolipid metabolism and postsynaptic glutaminergic signaling.

ACKNOWLEDGMENTS

The authors thank Dr. Christophe Poirier for providing mice with a deletion mutation in neutral sphingomyleinase-2 and Fang Yang for her technical assistance.

REFERENCES

Abulrob A, Tauskela JS, Mealing G, Brunette E, Faid K, Stanimirovic D. 2005. Protection by cholesterol-extracting cyclodextrins: a role for N-methyl-D-aspartate receptor redistribution. J Neurochem 92:1477–1486.

Aubin I, Adams CP, Opsahl S, Septier D, Bishop CE, Auge N, Salvayre R, Negre-Salvayre A, Goldberg M, Guenet JL, Poirier C. 2005. A deletion in the gene encoding sphingomyelin phosphodiesterase 3 (Smpd3) results in osteogenesis and dentinogenesis imperfecta in the mouse. Nat Genet 37:803–805.

Bajjalieh SM, Martin TF, Floor E. 1989. Synaptic vesicle ceramide kinase. A calcium-stimulated lipid kinase that co-purifies with brain synaptic vesicles. J Biol Chem 264:14354–14360.

Bandaru VV, McArthur JC, Sacktor N, Cutler RG, Knapp EL, Mattson MP, Haughey NJ. 2007. Associative and predictive biomarkers of dementia in HIV-1-infected patients. Neurology 68:1481–1487.

Bannerman DM, Good MA, Butcher SP, Ramsay M, Morris RG. 1995. Distinct components of spatial learning revealed by prior training and NMDA receptor blockade. Nature 378:182–186.

Besshoh S, Bawa D, Teves L, Wallace MC, Gurd JW. 2005. Increased phosphorylation and redistribution of NMDA receptors between synaptic lipid rafts and post-synaptic densities following transient global ischemia in the rat brain. J Neurochem 93:186–194.

Brann AB, Scott R, Neuberger Y, Abulafia D, Boldin S, Fainzilber M, Futerman AH. 1999. Ceramide signaling downstream of the p75 neurotrophin receptor mediates the effects of nerve growth factor on outgrowth of cultured hippocampal neurons. J Neurosci 19:8199–8206.

Clarke CJ, Hannun YA. 2006. Neutral sphingomyelinases and nSMase2: bridging the gaps. Biochim Biophys Acta 1758:1893–1901.

Claus RA, Dorer MJ, Bunck AC, Deigner HP. 2009. Inhibition of sphingomyelin hydrolysis: targeting the lipid mediator ceramide as a key regulator of cellular fate. Curr Med Chem 16:1978–2000.

Conrad CD, Galea LA, Kuroda Y, McEwen BS. 1996. Chronic stress impairs rat spatial memory on the Y maze, and this effect is blocked by tianeptine pretreatment. Behav Neurosci 110:1321–1334.

Coogan AN, O'Neill LA, O'Connor JJ. 1999. The P38 mitogen-activated protein kinase inhibitor SB203580 antagonizes the inhibitory effects of interleukin-1beta on long-term potentiation in the rat dentate gyrus in vitro. Neuroscience 93:57–69.

Crusio WE, Schwegler H. 2005. Learning spatial orientation tasks in the radial-maze and structural variation in the hippocampus in inbred mice. Behav Brain Funct 1:3.

Davis CN, Tabarean I, Gaidarova S, Behrens MM, Bartfai T. 2006. IL-1beta induces a MyD88-dependent and ceramide-mediated activation of Src in anterior hypothalamic neurons. J Neurochem 98:1379–1389.

Day CA, Kenworthy AK. 2009. Tracking microdomain dynamics in cell membranes. Biochim Biophys Acta 1788:245–253.

Dellu F, Fauchey V, Le Moal M, Simon H. 1997. Extension of a new two-trial memory task in the rat: influence of environmental context on recognition processes. Neurobiol Learn Mem 67:112–120.

Detre C, Kiss E, Varga Z, Ludanyi K, Paszty K, Enyedi A, Kovesdi D, Panyi G, Rajnavolgyi E, Matko J. 2006. Death or survival: membrane ceramide controls the fate and activation of antigen-specific T-cells depending on signal strength and duration. Cell Signal 18:294–306.

Fasano C, Miolan JP, Niel JP. 2003. Modulation by C2 ceramide of the nicotinic transmission within the coeliac ganglion in the rabbit. Neuroscience 116:753–759.

Frank C, Giammarioli AM, Pepponi R, Fiorentini C, Rufini S. 2004. Cholesterol perturbing agents inhibit NMDA-dependent calcium influx in rat hippocampal primary culture. FEBS Lett 566:25–29.

Fullekrug J, Simons K. 2004. Lipid rafts and apical membrane traffic. Ann N Y Acad Sci 1014:164–169.

Furukawa K, Mattson MP. 1998. The transcription factor NF-kappaB mediates increases in calcium currents and decreases in NMDA- and AMPA/kainate-induced currents induced by tumor necrosis factor-alpha in hippocampal neurons. J Neurochem 70:1876–1886.

Haughey NJ, Cutler RG, Tamara A, McArthur JC, Vargas DL, Pardo CA, Turchan J, Nath A, Mattson MP. 2004. Perturbation of sphingolipid metabolism and ceramide production in HIV-dementia. Ann Neurol 55:257–267.

Hering H, Lin CC, Sheng M. 2003. Lipid rafts in the maintenance of synapses, dendritic spines, and surface AMPA receptor stability. J Neurosci 23:3262–3271.

Hirata H, Hibasami H, Yoshida T, Ogawa M, Matsumoto M, Morita A, Uchida A. 2001. Nerve growth factor signaling of p75 induces differentiation and ceramide-mediated apoptosis in Schwann cells cultured from degenerating nerves. Glia 36:245–258.

Hofmann K, Tomiuk S, Wolff G, Stoffel W. 2000. Cloning and characterization of the mammalian brain-specific, Mg^{2+}-dependent neutral sphingomyelinase. Proc Natl Acad Sci U S A 97:5895–5900.

Inokuchi J, Mizutani A, Jimbo M, Usuki S, Yamagishi K, Mochizuki H, Muramoto K, Kobayashi K, Kuroda Y, Iwasaki K, Ohgami Y, Fujiwara M. 1997. Up-regulation of ganglioside biosynthesis, functional synapse formation, and memory retention by a synthetic ceramide analog (L-PDMP). Biochem Biophys Res Commun 237:595–600.

Ito A, Horigome K. 1995. Ceramide prevents neuronal programmed cell death induced by nerve growth factor deprivation. J Neurochem 65:463–466.

Kolmakova A, Kwiterovich P, Virgil D, Alaupovic P, Knight-Gibson C, Martin SF, Chatterjee S. 2004. Apolipoprotein C-I induces apoptosis in human aortic smooth muscle cells via recruiting neutral sphingomyelinase. Arterioscler Thromb Vasc Biol 24:264–269.

Lin Y, Skeberdis VA, Francesconi A, Bennett MV, Zukin RS. 2004. Postsynaptic density protein-95 regulates NMDA channel gating and surface expression. J Neurosci 24:10138–10148.

Luberto C, Hassler DF, Signorelli P, Okamoto Y, Sawai H, Boros E, Hazen-Martin DJ, Obeid LM, Hannun YA, Smith GK. 2002. Inhibition of tumor necrosis factor-induced cell death in MCF7 by a novel inhibitor of neutral sphingomyelinase. J Biol Chem 277:41128–41139.

Marchesini N, Hannun YA. 2004. Acid and neutral sphingomyelinases: roles and mechanisms of regulation. Biochem Cell Biol 82:27–44.

Melnikova T, Savonenko A, Wang Q, Liang X, Hand T, Wu L, Kaufmann WE, Vehmas A, Andreasson KI. 2006. Cycloxygenase-2 activity promotes cognitive deficits but not increased amyloid burden in a model of Alzheimer's disease in a sex-dimorphic pattern. Neuroscience 141:1149–1162.

Mizutani Y, Tamiya-Koizumi K, Irie F, Hirabayashi Y, Miwa M, Yoshida S. 2000. Cloning and expression of rat neutral sphingomyelinase: enzymological characterization and identification of essential histidine residues. Biochim Biophys Acta 1485:236–246.

Nakazawa K, McHugh TJ, Wilson MA, Tonegawa S. 2004. NMDA receptors, place cells and hippocampal spatial memory. Nat Rev Neurosci 5:361–372.

Nicol GD. 2008. Nerve growth factor, sphingomyelins, and sensitization in sensory neurons. Sheng Li Xue Bao 60:603–604.

Numakawa T, Nakayama H, Suzuki S, Kubo T, Nara F, Numakawa Y, Yokomaku D, Araki T, Ishimoto T, Ogura A, Taguchi T. 2003. Nerve growth factor-induced glutamate release is via p75 receptor, ceramide, and Ca^{2+} from ryanodine receptor in developing cerebellar neurons. J Biol Chem 278:41259–41269.

Owen DM, Williamson D, Rentero C, Gaus K. 2009. Quantitative microscopy: protein dynamics and membrane organisation. Traffic 10: 962–971.

Peng CH, Huang CN, Hsu SP, Wang CJ. 2006. Penta-acetyl geniposide induce apoptosis in C6 glioma cells by modulating the activation of neutral sphingomyelinase-induced p75 nerve growth factor receptor and protein kinase Cdelta pathway. Mol Pharmacol 70:997–1004.

Rao BG, Spence MW. 1976. Sphingomyelinase activity at pH 7.4 in human brain and a comparison to activity at pH 5.0. J Lipid Res 17:506–515.

Rogasevskaia T, Coorssen JR. 2006. Sphingomyelin-enriched microdomains define the efficiency of native Ca^{2+}-triggered membrane fusion. J Cell Sci 119:2688–2694.

Rohrbough J, Rushton E, Palanker L, Woodruff E, Matthies HJ, Acharya U, Acharya JK, Broadie K. 2004. Ceramidase regulates synaptic vesicle exocytosis and trafficking. J Neurosci 24:7789–7803.

Savonenko A, Xu GM, Melnikova T, Morton JL, Gonzales V, Wong MP, Price DL, Tang F, Markowska AL, Borchelt DR. 2005. Episodic-like memory deficits in the APPswe/PS1dE9 mouse model of Alzheimer's disease: relationships to beta-amyloid deposition and neurotransmitter abnormalities. Neurobiol Dis 18:602–617.

Schneider PB, Kennedy EP. 1967. Sphingomyelinase in normal human spleens and in spleens from subjects with Niemann-Pick disease. J Lipid Res 8:202–209.

Schwegler H, Boldyreva M, Linke R, Wu J, Zilles K, Crusio WE. 1996. Genetic variation in the morphology of the septo-hippocampal cholinergic and GABAergic systems in mice: II. Morpho-behavioral correlations. Hippocampus 6:535–545.

Shaikh NA. 1994. Assessment of various techniques for the quantitative extraction of lysophospholipids from myocardial tissues. Anal Biochem 216:313–321.

Sipka S, Antal-Szalmas P, Szollosi I, Csipo I, Lakos G, Szegedi G. 2000. Ceramide stimulates the uptake of neutral red in human neutrophils, monocytes, and lymphocytes. Ann Hematol 79:83–85.

Smith AR, Visioli F, Frei B, Hagen TM. 2006. Age-related changes in endothelial nitric oxide synthase phosphorylation and nitric oxide dependent vasodilation: evidence for a novel mechanism involving sphingomyelinase and ceramide-activated phosphatase 2A. Aging Cell 5:391–400.

Stahelin RV. 2009. Lipid binding domains: more than simple lipid effectors. J Lipid Res 50(Suppl):S299–S304.

Steele RJ, Morris RG. 1999. Delay-dependent impairment of a matching-to-place task with chronic and intrahippocampal infusion of the NMDA-antagonist D-AP5. Hippocampus 9:118–136.

Stoffel W, Jenke B, Block B, Zumbansen M, Koebke J. 2005. Neutral sphingomyelinase 2 (smpd3) in the control of postnatal growth and development. Proc Natl Acad Sci U S A 102:4554–4559.

Stoffel W, Jenke B, Holz B, Binczek E, Gunter RH, Knifka J, Koebke J, Niehoff A. 2007. Neutral sphingomyelinase (SMPD3) deficiency causes a novel form of chondrodysplasia and dwarfism that is rescued by Col2A1-driven smpd3 transgene expression. Am J Pathol 171:153–161.

Swartz KJ. 2008. Sensing voltage across lipid membranes. Nature 456: 891–897.

Tabarean IV, Korn H, Bartfai T. 2006. Interleukin-1beta induces hyperpolarization and modulates synaptic inhibition in preoptic and anterior hypothalamic neurons. Neuroscience 141:1685–1695.

Takahashi E, Inanami O, Asanuma T, Kuwabara M. 2006. Effects of ceramide inhibition on radiation-induced apoptosis in human leukemia MOLT-4 cells. J Radiat Res 47:19–25.

Tomiuk S, Hofmann K, Nix M, Zumbansen M, Stoffel W. 1998. Cloned mammalian neutral sphingomyelinase: functions in sphingolipid signaling? Proc Natl Acad Sci U S A 95:3638–3643.

van Blitterswijk WJ, van der Luit AH, Veldman RJ, Verheij M, Borst J. 2003. Ceramide: second messenger or modulator of membrane structure and dynamics? Biochem J 369:199–211.

Walton KA, Gugiu BG, Thomas M, Basseri RJ, Eliav DR, Salomon RG, Berliner JA. 2006. A role for neutral sphingomyelinase activation in the inhibition of LPS action by phospholipid oxidation products. J Lipid Res 47:1967–1974.

Wheeler D, Knapp E, Bandaru VV, Wang Y, Knorr D, Poirier C, Mattson MP, Geiger JD, Haughey NJ. 2009. Tumor necrosis factor-alpha-induced neutral sphingomyelinase-2 modulates synaptic plasticity by controlling the membrane insertion of NMDA receptors. J Neurochem 109:1237–1249.

Yamagishi K, Mishima K, Ohgami Y, Iwasaki K, Jimbo M, Masuda H, Igarashi Y, Inokuchi J, Fujiwara M. 2003. A synthetic ceramide analog ameliorates spatial cognition deficit and stimulates biosynthesis of brain gangliosides in rats with cerebral ischemia. Eur J Pharmacol 462:53–60.

Yang SN. 2000. Ceramide-induced sustained depression of synaptic currents mediated by ionotropic glutamate receptors in the hippocampus: an essential role of postsynaptic protein phosphatases. Neuroscience 96:253–258.

Yu SP, Yeh CH, Gottron F, Wang X, Grabb MC, Choi DW. 1999. Role of the outward delayed rectifier K^+ current in ceramide-induced caspase activation and apoptosis in cultured cortical neurons. J Neurochem 73:933–941.

Zhang YH, Nicol GD. 2004. NGF-mediated sensitization of the excitability of rat sensory neurons is prevented by a blocking antibody to the p75 neurotrophin receptor. Neurosci Lett 366:187–192.

Zhang YH, Vasko MR, Nicol GD. 2002. Ceramide, a putative second messenger for nerve growth factor, modulates the TTX-resistant Na^+ current and delayed rectifier K^+ current in rat sensory neurons. J Physiol 544:385–402.